

VIBRO-IMPACTS INDUCED BY IRREGULAR ROLLING SURFACES OF RAILWAY RAILS AND WHEELS

ZOFIA KOWALSKA

Institute of Fundamental Technological Problems PAS, Warsaw, Poland

e-mail: zkowal@ippt.gov.pl

Irregularities on rolling surfaces of deformable compact bodies induce normal contact vibrations and vibro-impacts in particular. Modelling, simulation and analysis of such an excitation and the system dynamical response are the objects of the study. Parameter analysis of transient vibro-impacts induced by a single irregularity is helpful in the understanding of dynamical properties of the system. Moreover, the analysis may be helpful in experiment design for detecting defects of rolling surfaces and faults of neighbour structures suspending/supporting the rolling bodies. Simulations performed with very simple models are next compared with results obtained from simulations of the whole wagon performed by using the Adams/Rail software.

Key words: unilateral contact, contact vibration, wheel-rail contact

1. Introduction

Two compact hard bodies in unilateral rolling contact constitute the core of the studied systems. Dynamical behaviour of the core system depends on its parameters, rolling surface geometry and also on dynamical properties of the adjoining structures. A simple example shown in Fig. 1a consists of a flexibly suspended rolling body m pressed against an elastic half-space with an additional external force P . Under certain conditions, such a system is a reduced model of the wheel/rail system. Normal contact vibrations and vibro-impacts excited with irregularities on the rolling surfaces are of interest. The systems of this type are also encountered in other engineering systems. Examples include: a cam and a roller, a ball and its race in rolling bearings.

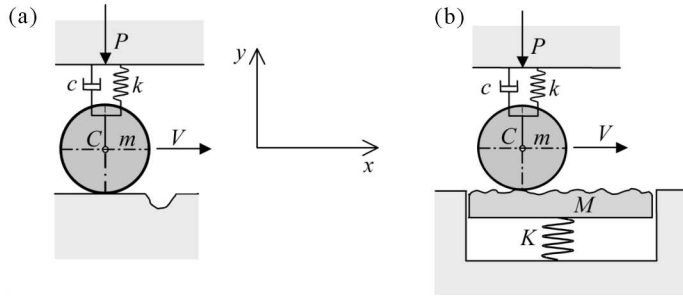


Fig. 1. Simple models: (a) unsprung mass m of the wheelset and its primary suspension k - c on a stiff foundation, (b) the same system rolling over the floating deck of the railroad scale

The main objective of the investigation is to gain a better insight into the system dynamics, in particular to understand how the adjoining structures, namely the suspension and support, influence the dynamics of the above described core system. The practical objective is to investigate via computer simulation the possibility of wayside detection of wheelset defects in train motion. Particular defects are of interest, for example: a broken spring in the primary suspension, bad fixing of ends of the springs or dampers.

2. Modelling and simulation

The main assumption in the modelling is that the bodies are infinitely rigid, only a finite contact compliance of curved rolling surfaces is taken into account. The system structure changes whenever the sign of indentation δ changes from positive to negative or vice versa. At every step of numerical integrations the current value of indentation is computed. The systems of this type are very sensitive to errors in values of times at which the structure of the system changes (Bogacz and Kowalska, 2001).

In the case of the system m - c - k rolling over the floating deck M , the indentation δ is a sum of the rolling body displacement $-y_C$ and the floating deck displacement y_M as well as the constraint y_C^k

$$\delta = -y_C + y_C^k + y_M \geq 0 \quad (2.1)$$

The constraint $y_C^k(x)$ is a trajectory of the centre C (see Fig. 1) in the case when both bodies are in contact and are infinitely rigid. In the two-dimensional (plane) problem, for a given profile of the surface $y_r(x)$, the value of constraint at a given abscissa $y_C^k(x_0)$ is calculated from the formula

$$y_C^k(x_0) = \sqrt{R^2 - (x - x_0)^2} + y_r(x) \quad \text{for } x = x_c \quad (2.2)$$

where x_c denotes the horizontal coordinate of the contact point of the circle of radius R and the profile. The value x_c is numerically determined by maximizing the sum in formula (2.2) with respect to x . It is a sum of a half of the vertical chord on the line $x = x_c$ and the value of the profile height $y_r(x)$ at $x = x_c$. In other words, we look for the point where the gap between the circle and the profile is minimal, and is equal to zero (Bogacz and Kowalska, 2001).

When the bodies are in contact, their vertical motion is governed by equations

$$\begin{aligned} m\ddot{y}_C &= -P - mg - ky_C - c\dot{y}_C + N(\delta) \cos \alpha \\ M\ddot{y}_M &= -N(\delta) \cos \alpha - Mg - Ky_M \end{aligned} \quad (2.3)$$

In the systems being considered, the angle α is very small and $\cos \alpha \approx 1$. The relationship $N(\delta)$ is referred to as a static contact model. In the elastic range, a Hertzian model is used, that is $N(\delta) = C\sqrt{\delta^3}$, and the coefficient C changes with the curvature of the irregularity $y_r(x)$. Thus, two types of excitations take place, a displacement excitation modelled with the constraint and a parametric excitation due to changes in the contact stiffness. In the elastic-plastic range, Johnson's indentation model is used (Johnson, 1985; Stronge, 2000); the loading characteristic to compute motion and the unloading characteristics to compute permanent patterns left on the rolling surfaces in result of vertical oscillations (Kowalska, 2004).

3. Systems properties

The systems under consideration are inherently non-linear and show, in general, very complex dynamical behaviour. Herein, the analysis is focused on transient vibro-impacts excited with a single irregularity of a cosine profile. Figure 2a presents an exemplary transient dynamical response $N(t)$ of a heavily damped rolling system on a stiff foundation. The time history $N(t)$ of the normal contact force shows two phases: the initial phase of vibro-impacts, and the phase of subsequent normal contact vibrations.

In dynamical analysis, the level surfaces of chosen scalar features of a dynamic response were used. Such an analysis helps to improve the parameterisation of the model, in particular helps to avoid parameter redundancy, and to find measurable features which are the most sensitive and specific for

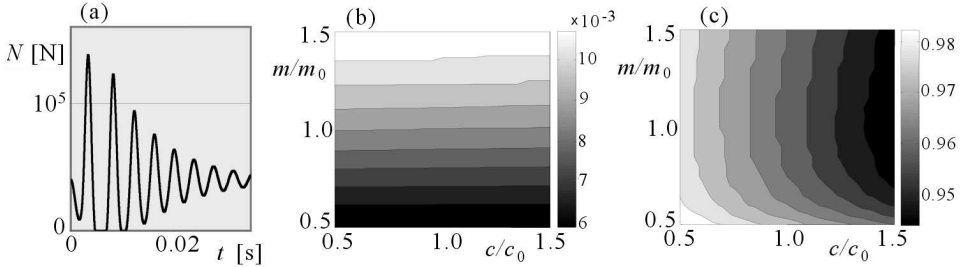


Fig. 2. Transient responses: (a) exemplary time history $N(t)$; (b) level curves of the time distance Δt ; (c) level curves of the normal forces ratio r_N

a chosen parameter. In turn, the parameter estimation is helpful in defects diagnostics. For example, Figs. 2b and 2c show the level curves of two scalar features on the xy -plane, where $x = c/c_0$, $y = m/m_0$ and m_0 , c_0 denote the nominal values of the damping coefficient c and mass m . The mentioned features are: the time distance Δt between two subsequent impacts (Fig. 2b) and the ratio r_N of the maximum normal forces at two subsequent impacts: $N_{\max(i-1)}/N_{\max i}$ (Fig. 2c). In the first case, the gradient vectors on the level curves are almost parallel to the m/m_0 -axis, which indicates that the time period Δt is a very specific feature for the mass m . In a relatively large neighbourhood of the point $(1, 1)$, the ratio r_N is also specific for the damping coefficient c in the suspension.

In the system with the floating deck (Fig. 1b), vibrations induced with irregularities on the rolling surface are sensitive to parameters of the rolling system: m - c - k . In particular, a fundamental frequency of transient vibrations is sensitive to m and the rate of decrease of the amplitude of oscillations is sensitive to the damping coefficient c . Generally, the tendency of the rolling body to bounce after the excitation with irregularity of a given amplitude decreases with a decrease of the dynamic stiffness of the foundation. The magnitude of the dynamic stiffness equals: $M\omega^2 + C\omega + K$, where C and K denote damping and stiffness of the floating deck bearing. Moreover, the maximum normal force N_{\max} decreases with the dynamic stiffness decrease.

4. Simulations with Adams/Rail software

Since several years, owing to rapid development of computer technology, the so called "computational railway dynamics" has been developing very fast as well. Presently, many research groups investigate numerous important theoretical

and practical problems using very complex computer models of railway wagons and tracks. The Adams/Rail software is one of the most popular modelling tool in which well-established models of sub-systems are implemented. However, the question of unilateral dynamical contact has not been sufficiently examined yet.

One of the reasons of this state of art is that it is easy to overlook short loses of contact when inappropriate numerical integrators are used in simulations. According to Bogacz and Kowalska (2001), the loses of contact are very likely at high train speeds in the case of short periodic rail irregularities, which are called corrugations. In a few earlier publications, for example Nielsen and Igeland (1995), Ilias (1996), Igeland and Ilias (1997), the authors explored problems of modelling and computational analysis of the dynamic contact of a railway wheel with a corrugated rail. However, they dealt with bilateral contact. On the other hand, it is worth to mention the paper by Nayak (1972), who more than thirty years ago noticed the problem of unilateral wheel/rail contact. He investigated the dynamics of the core system shown in Fig. 1a using analytical but approximate methods of non-linear vibration analysis.

A series of simulations of the whole wagon were performed using the Adams/Rail program. The practical aim and motivation of simulations was to find those measurable signals whose properties are sensitive and specific for particular defects of a wheelset or its suspension, and for that reason the signals could be useful in dynamical diagnostics performed in train motion.

In the Adams/Rail program, motion of the whole ERRI virtual wagon is simulated. The ERRI stands for European Rail Research Institute, and the ERRI wagon was developed as a benchmark for evaluating computer software. It has a structure and parameters of a common modern railway passenger wagon. The car body of the ERRI wagon is supported by two bogies (Fig. 3). Springs and dampers between the car body and frame of the bogie create the secondary suspension. Both rear and front bogies consist of two wheelsets. Each wheelset is connected with a frame through dampers and springs that constitute the so-called primary suspensions. The original ERRI wagon is equipped with dampers whose parameters and characteristics can be easily changed. Results given herein are obtained for damping-free wagon; therefore we can observe long-lasting transients. The only sources of damping are frictional damping, calculated by Kalker theory (Kalker, 1991), and material damping in the contact zones. In this Section simulations of transients induced by single short irregularities are discussed.

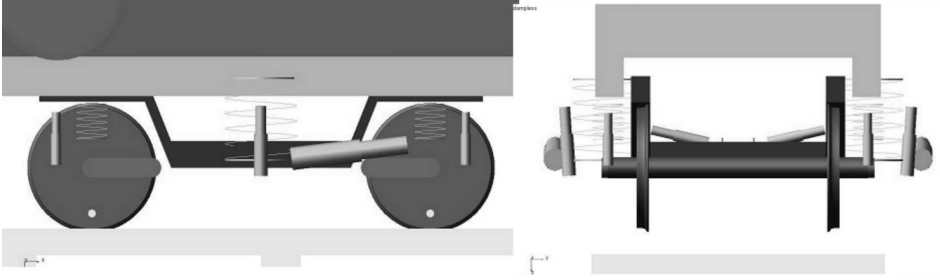


Fig. 3. Side and rear view of the bogie supporting a car body of the ERRI wagon

Simulations performed with the Adams/Rail software generally confirmed that a simple model consisting of an effective mass m and a damper c is a good approximate model to simulate transient vertical vibro-impacts in the case of an impulse excitation with identical vertical irregularities on both rails or wheels. The spring representing the stiffness k of the primary suspension is of lesser importance. In other words, the transients are almost insensitive to the spring stiffness k due to its relatively low value.

Figure 4 shows a response to the step excitation of the front and rear wheelset of the same bogie. The notation is as follows: N denotes normal force, T denotes lateral force. The letters ' f ' and ' r ' stand for *front* and *rear*, and the letters ' R ' and ' L ' stand for *right* and *left*. First, the front wheelset is excited, next the rear one. It can be seen that vertical motion of the front wheelset is not affected by the excitation of the rear wheelset. Other simulations also confirm that vertical motion of the wheelset is practically uncoupled with vertical motion of the second wheelset of the same bogie. Contact vibrations of a frequency about 200 Hz are not transmitted through the sub-system of a heavy mass of the wheelset and its soft primary suspension.

For comparison, the lateral forces are shown in Fig. 4 as well. Despite a symmetrical excitation, the lateral forces do not equal zero because the wheel and rail profiles are designed so that the normal force has a very small component directed toward the centre line of the track, and some frictional forces are also involved.

The situation is a bit different in the case of irregularities on one rail or one wheel. In such a case, vertical oscillations of the wheelset are coupled with angular oscillations around its mass centre, and due to higher frictional forces both lateral and vertical oscillations are more strongly damped. Moreover, transient normal forces on the right and left site are not in phase.

Figure 5 shows the normal contact forces and the acceleration of the mass centre of the floating deck (see Fig. 1b). The vibro-impacts are excited with

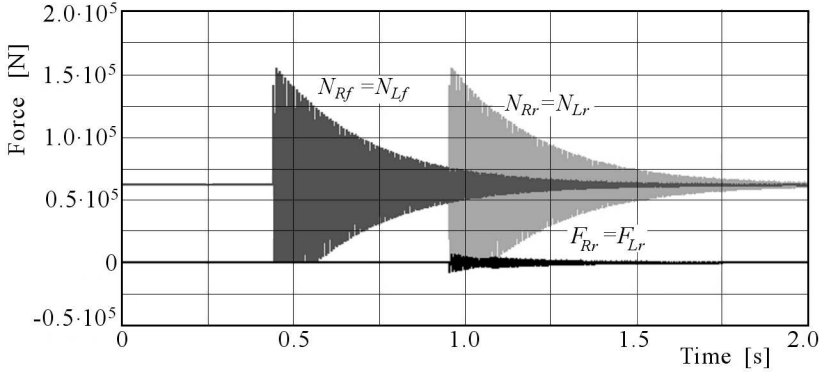


Fig. 4. Normal and lateral forces resulting from a step excitation on both rails

flats on the wheels of a depth (strictly speaking – a sagitta) 0.1 mm. The flats on the wheels usually result from sliding of the wheels on rails, which is caused by an emergency over-braking with blocked wheels. The flat is a source of a displacement excitation expressed with the constraint y_C^k . In this case, the constraint means a change in the relative vertical distance between two points of a rigid wheel rolling on the rigid floating deck. The contact stiffness changes when the flattened wheel rolls along a rail. This additional parametric excitation has been neglected because the Adams/Rail software does not model such an excitation yet. However, simulations of transients with the core system model show that this parametric excitation is much less significant than the displacement excitation and, therefore, can be neglected.

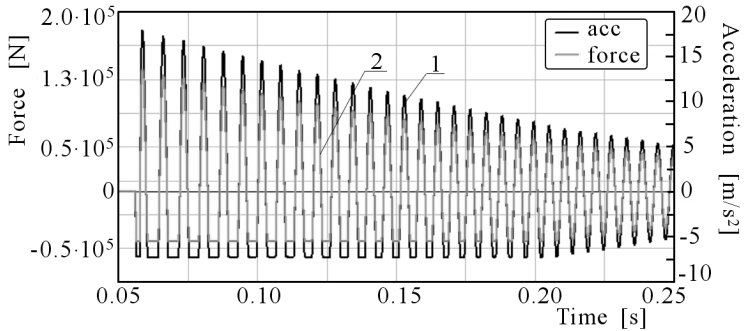


Fig. 5. Dynamical response to an excitation with flats of the sagitta 0.1 mm on both wheels at the velocity 5 m/s: 1 – dynamical component of the normal force, 2 – acceleration

In this example, the mass M of the floating desk is ten times larger than the mass m of the wheelset, and $m = 1500$ kg. The first observation, which

is not illustrated herein, is that for such a big mass M and for frequencies of 100-200 Hz – that is frequencies of contact vibrations and transient vibro-impacts – the normal forces are practically identical as for the stiff track. In Fig. 4, we can see that the acceleration $\ddot{y}_M(t)$ of the heavy floating deck reflects the time history of the normal force $N(t)$ very well. In fact, in this case, the acceleration is almost linearly proportional to the force.

Figure 6 illustrates how the step irregularity of a depth 0.1 mm affects the ride comfort measured with the acceleration of the mass centre of the car body. In the case of a damping-free wagon without any dampers or other sources of damping in the primary or secondary suspension, the step irregularity excites non-damped oscillations of very low amplitudes. In the case of the original ERRI wagon, the impulse excitation causes a short jerk the amplitude of which is even higher than without the damping. Despite a small velocity $V = 5$ m/s, for short irregularities the dampers are harmful. However, in both cases, the vertical accelerations are very small and we can say that short irregularities do not affect the ride comfort but they may cause very high contact forces which badly affect wear of the wheels and rails.

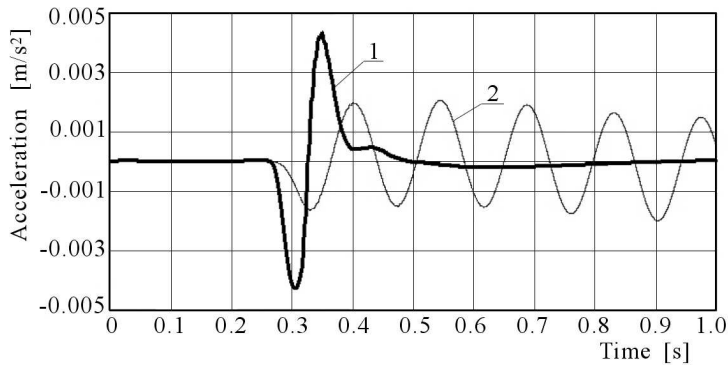


Fig. 6. Dynamical response to an excitation with a step irregularity of the depth 0.1 mm at the velocity 5 m/s: 1 – ERRI original wagon, 2 – ERRI damping-free wagon

5. Vibro-impact induced by periodic irregularities

In this Section, the dynamical response of the rear wheelset of the rear bogie of the ERRI wagon to excitations with a harmonic rail irregularity is discussed. Simulations with sinusoidal excitations are intended to get a better insight into the dynamics of the system. Moreover, they are helpful in the analy-

sis of damage mechanism leading to corrugations on rail and wheel surfaces. Corrugations are periodic irregularities of a period of several centimetres.

The irregularity is given in the form: $y_r(t) = -a \sin[(x - x_0)2\pi/\lambda]$ for $x \geq x_0$. The simulations were performed with the Adams/Rail software. The sinusoidal irregularity starts at a distance x_0 from the beginning of a virtual track, at the point which is between the front and the rear wheelset of the rear bogie at the time $t = 0$.

Typical results of simulations are given in Fig. 7. Values of parameters of the sinusoidal excitation are as follows: the amplitude a is $50 \mu\text{m}$, the period λ is 5 cm and the velocities V of the ERRI wagon are: 2.25 m/s, 9 m/s, and 36 m/s, that is, respectively: 8.1 km/h, 32.4 km/h and 129.6 km/h. When the period $\lambda = 5$ cm and the amplitude $50 \mu\text{m}$ or less, then the constraint $y_C^k(t)$ is almost identical with the rail irregularity $y_r(t)$. Therefore, for simplicity, in the text and in the graphs, the two terms, i.e. irregularity and constraint, are used synonymously. The frequency of the harmonic excitation equals $f_s = V/\lambda$.

Each of the three graphs in Fig. 7 illustrates different operational conditions. The upper one – a very low velocity V of the wagon and f_s far below the contact resonance region, the middle one – a low velocity of the wagon, the contact resonance region, and the lower graph – medium and high velocity and far above the resonance region.

There are three curves in each graph: 1 – the irregularity $y_r(t)$, 2 – the variable component of the vertical displacement of the centre of mass (CM) of the rear wheelset in the rear bogie $y_C(t)$, 3 – the normal force $N(t)$.

For a low velocity and a low frequency of excitation, after transient motion decays, the variable component of CM displacement $y_C(t)$ has almost identical amplitude as the irregularity $y_r(t)$ and is in-phase with the irregularity. In the upper graph, after some time from the beginning of excitation, the curve $y_C(t)$ overlays the curve $y_r(t)$. The variable component of the normal force is small, harmonic and is in anti-phase with the irregularity. Physically, it is better to say that the acceleration of CM is in-phase with the normal force. Thus, in this region of frequency, the bodies in contact behave similarly to the rigid ones.

When the frequency of sinusoidal excitation $f_s = V/\lambda$ is about the contact resonance frequency f_r , then high bounces of the wheelset are observed. Maximum values of the normal force $N(t)$ are several times greater than the normal static load. Maximum values of the vertical displacements $y_C(t)$ of the wheelset CM are also very high, as high as 1 mm and even more. It is seen in Fig. 7 that at resonance, the vertical position $y_C(t)$ of CM rises very quickly.

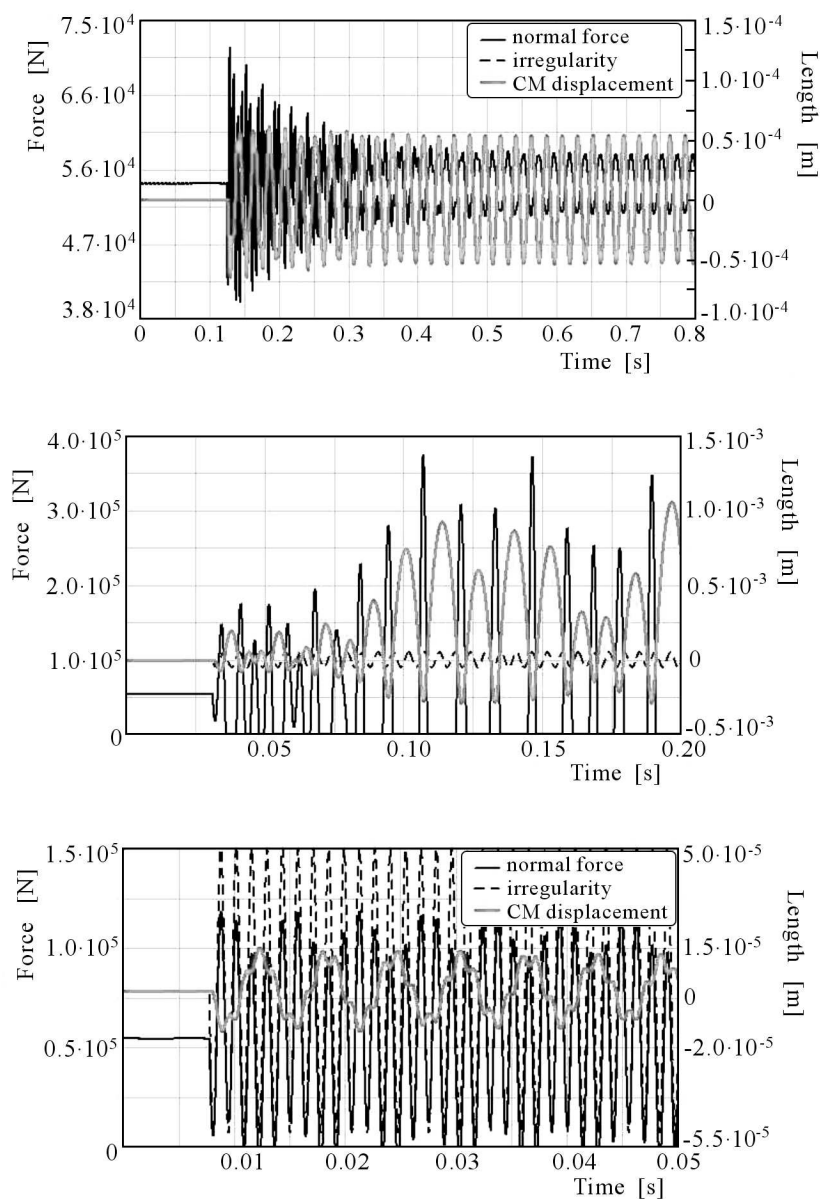


Fig. 7. Dynamical response of the rear wheelset to an excitation with a sinusoidal irregularity on both rails of the amplitude $50\ \mu\text{m}$ and the period $5\ \text{cm}$: upper – below the resonance regime at velocity $2.25\ \text{m/s}$; middle – close to the resonance frequency at velocity $9\ \text{m/s}$; lower – above the resonance regime at the velocity $36\ \text{m/s}$

For an amplitude of $50\ \mu\text{m}$ within only a half of the period of excitation, the wheelset bounces off the rails. The time distance between subsequent impacts of the wheels on rails depends on the bounce height, but generally is longer than the period λ/V . For a given irregularity, the height of bounces depends on the wheelset mass m and the static normal load P . At resonance, time histories $y_C(t)$, $N(t)$ are complex mainly due to the unilateral type of contact. The non-linearity of contact stiffness is of lesser importance. After a long time period since the beginning of sinusoidal excitations, limiting cycles are observed, but they have not been fully examined yet.

At higher velocities or higher frequencies of the excitation, that is far above the resonance region, different time patterns of oscillations are observed. The amplitude of displacement of the wheelset CM is significantly less than the amplitude of the irregularity. The wheel compresses the irregularity peaks and does not go into its valleys. Physically, it can be explained as follows: at high frequencies of the excitation, the wheelset is too heavy (its mechanical impedance is too high) to follow the irregularities. However, in the post-resonance regime, instantaneous values of normal forces are high, much higher than the static load, although the amplitude of the wheelset CM displacement decreases in time for a given velocity V and also decreases with the velocity increase. High instantaneous values of the normal force are at peaks and low or zero at valleys.

Notice that the simulations performed with the core system model revealed the same oscillatory time patterns in three frequency ranges (Bogacz and Kowalska, 2001). In other words, dynamical properties of the core system are preserved in the complex system. This means that dynamical couplings between the core system and the adjacent dynamical structures are weak.

The weakness of dynamical coupling between vertical oscillations of two wheelsets of the same boogie has been already illustrated with the step response of the system in Fig. 4. Generally, a dynamical response to periodic excitation gives more information of any system dynamics than the impulse or step response. Therefore, another simulation experiment was performed. Figure 8 presents vertical oscillations of the rear wheelset and the bogie frame at the velocity $V = 18\ \text{m/s}$. The front wheelset encounters first sinusoidal irregularities on both rails at the time $t \approx 0.1\ \text{s}$. Vertical motion of the front wheelset also slightly excites the bogie frame. Its motion is normally damped, but in this simulation experiment all damping sources were deactivated in order to better grasp the inertial couplings. After some time, the rear wheelset encounters the beginning of sinusoidal irregularity, and then transients of high amplitude are observed. We can see that oscillations of the rear wheelsets

start before it encounters the beginning of the sinusoidal irregularity, but the amplitude of these oscillations is very small, almost unnoticeable. Generally, contact vibrations or vibro-impacts excited with surface irregularities are effectively filtered out by a heavy mass of the wheelset suspended by means of a relatively soft primary suspension.

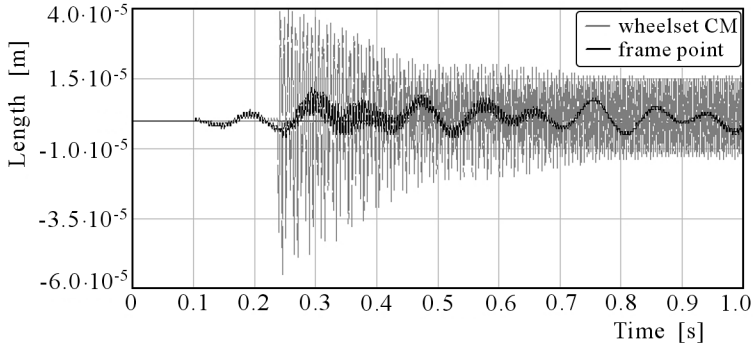


Fig. 8. Vertical vibrations of the rear wheelset CM and the bogie frame point above the wheelset CM

At the end, let us consider the case when the sinusoidal irregularity is applied to the right rail only. When comparing the graph of the right normal force in Fig. 9 with the graph of the force in the post-resonance regime in Fig. 7, we can see that time histories of the forces are very similar. The reason of such conformity is as follows. In both considered cases, motion of the wheel centre is smooth in comparison with harmonic constraints. Therefore, the normal force time pattern results primarily from the elastic pressing of sinusoidal irregularities by the smoothly rolling wheel. In the second case, only the right wheel rolls over irregularities. It presses the peaks, and it is seen in the normal force time history, which contains a frequency component equal to the frequency constraints. The left normal force in Fig. 9 contains only a lower frequency component of a smaller amplitude.

Figure 10 compares vertical motion of the left and right wheel CM in the case of excitation on the right rail only. The amplitudes at the velocity $V = 36 \text{ m/s}$ are very small in comparison with the amplitude of irregularity $a = 50 \mu\text{m}$. In the time history of motion of the centre of the right wheel, the component of corrugations is seen, which is entirely filtered out on the left side. After a short time from the beginning, the centres of both wheels move in phase upwards and downwards. This mode of vibrations dominates in wheelset motion, despite the unsymmetrical excitation. Other possible modes of the

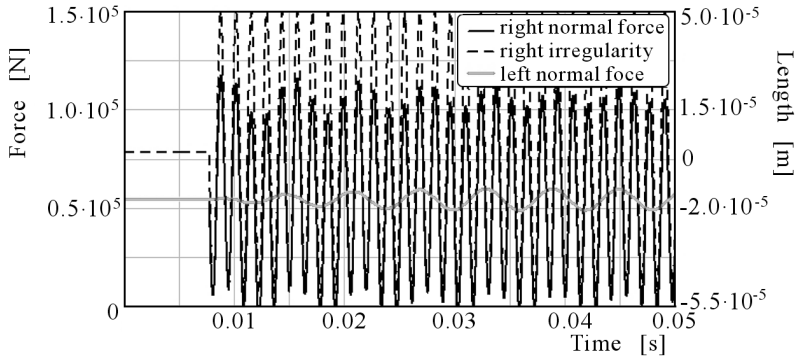


Fig. 9. Right and left normal forces in the post-resonance regime for an excitation with a sinusoidal irregularity on the right rail

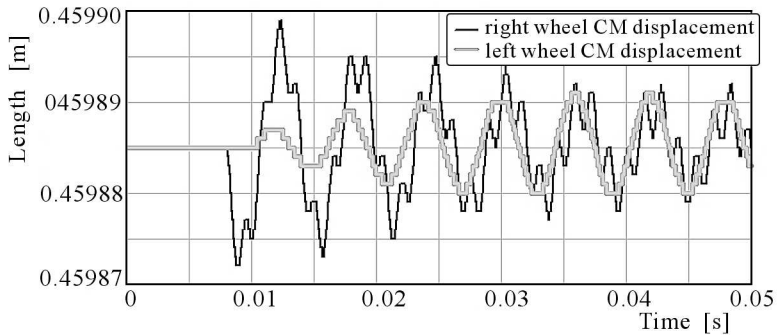


Fig. 10. Displacements of the centres of the left and right wheel for an excitation with a sinusoidal irregularity on the right rail

wheelset oscillations, that is lateral motion or angular oscillations around the wheelset CM, are damped by tangential frictional forces. Moreover, angular oscillations of the wheelset in the ERRI wagon are very much constrained by its mechanical structure: the wheelset together with parallel rigid links joining the axle boxes with the bogie frame, form the so-called trailer.

6. Conclusions

In addition to the results discussed and illustrated above, the simulations performed with the Adams/Rail software and the simple models given in Fig. 1 have revealed some dynamical properties of the considered system and have lead us to the following conclusions.

The simple models shown in Fig. 1 and discussed in Section 1 and 2 are appropriate for basic analysis of vibro-impacts induced by short single or periodic irregularities, particularly in cases when the irregularities are the same on both wheels or rails. This is because the properties of isolated sub-systems determine dynamical behaviour of the whole system. Vibro-impacts of a relatively high frequency excited in the wheel/rail contact zone are effectively filtered out by the mechanical filter consisting of a wheelset and its soft primary suspension. A small amount of vibration energy can be transmitted to the bogie frame but practically is not transmitted to the car body through the secondary suspension. That is why the simple model (see Fig. 1a) can be accepted as a reduced model of a complex system in the case of a stiff railway track.

A disadvantage of the Adams/Rail model of the wheel/rail contact is the fact that the contact compliance does not depend on the profile $y_r(t)$ – it is always the same as for a smooth rail and wheel. In fact, the model involves only the displacement excitation with the constraint and neglects parametric excitation due to changes in the contact stiffness. The advantage of the Adams/Rail model as compared with the simple models given in Fig. 1 is that it comprises the model of frictional contact forces based on Kalker's theory (Kalker, 1991). This is particularly important in simulations of the dynamical response to the excitation with the irregularity on one rail or wheel only. In such cases, transients are usually shorter due to higher frictional forces in the contact zone.

Let us consider practical aspects of dynamical properties discussed above in respect of damage of the wheel and rail.

For the wheelset mass equal to 1500 kg the contact resonance frequency f_r is about 180 Hz. Hence, for a sinusoidal irregularity of the period $\lambda = 5$ cm, the velocity V at which the contact resonance occurs is slightly above 30 km/s, whereas for the period 10 cm, the relevant velocity is about 60 km/s. It means that practically in normal straight-line motion all modern trains operate in post-resonance conditions. The resonance conditions also occur, but less frequently, when accelerating or slowing down.

In simulations with the Adams/Rail the model of the contact zone is purely elastic, however at forces as high as twice greater than the static load the limits of elastic behaviour are exceeded and some permanent deformations due to plastic flow are unavoidable. Thus, it can be expected that the wheel rolling or bouncing over a smooth or corrugated rail can change the rail and wheel profiles due to plastic deformations. Moreover, it can initiate or develop cracking.

In respect of fatigue damage, the fact that trains normally operate in post-resonance conditions is disadvantageous because high normal forces are impossible to avoid. The consequences of these dynamical properties depend on the quality of steel that is on the main failure mechanism of wheels and rails. It seems that a ductile rail with a hard surface layer of high fatigue strength bears such dynamical loading well and plastic deformations due to high forces at peaks may even help to smooth irregularities. However, when mechanical fatigue is the main mechanism of failure, high normal forces in the post-resonance region accelerate damage of wheels and rails.

Dynamical response $N(t)$ to a single irregularity on a stiff track consists of a long series of impacts. So, a long section of the rail undergoes hammering and is prone to fatigue damage. In this respect a flexible track is better than a stiff track. However, it is impossible to attenuate even on a flexible track the first and the highest impulse of the normal force induced by a short irregularity.

Let us sum up the main results which consist the basis for design of railway diagnostic systems. Time histories of normal forces $N(t)$ on a stiff track are sensitive to different defects of wheelsets and their primary suspension. Some faults generate transients or periodic signals $N(t)$ of a specific time pattern. Other faults can be detected from transients excited with specially designed irregularities put purposely on the rails of the test track. The frequency of transient vibro-impacts strongly depends on the effective value of the unsprung mass m . Some defects may change the effective unsprung mass. For instance, a broken spring of the primary suspension may result in a quasi-rigid connection between the wheelset and the bogie frame, and it can be detected by measuring the frequency of a transient vibro-impact.

Easy measurable vertical acceleration $\ddot{y}_M(t)$ of the heavy 'floating deck', which is supported on relatively soft bearings of the stiffness K , imitate very well the time-history of normal contact forces $N(t)$, therefore measurements of the acceleration can be used for diagnostic purposes.

Direct measurements of the contact forces are nowadays impossible. However, the signal of vertical forces can be extracted from the acceleration signal of a heavy floating deck. Note, that the elastic support of the floating deck should be pre-stressed with a load equal to the vertical static force, when the wheelset of interest approaches the floating deck.

In general, the simulations prove the possibility to develop a test railway track for efficient diagnostics of wheelsets in train motion. Different technical problems need to be solved, but they are solvable at the present stage of measuring technology.

In regards of diagnostic systems for detection of track faults, in particular for detection of short irregularities on rails, dynamical properties of the system under study are not advantageous. Short irregularities do not affect the bogie ride quality much, but profoundly affect the contact forces and noise. The main component of motion $y_C(t)$ with bounces has a lower frequency than the irregularity $y_r(t)$. Bounces may also contain higher components, which do not exist in the spectrum of irregularity. The differences in time histories $y_r(t)$, $y_C(t)$ and their spectra are important when designing a track diagnostic system based on measurements of accelerations $\ddot{y}_C(t)$. Such a diagnostic assessment can be misleading or limited.

Acknowledgements

This work was supported by the Polish Ministry of Scientific Research and Information Technology (MNI Grant No. 5 T12 C019 24).

References

1. BOGACZ R., KOWALSKA Z., 2001, Computer simulation of interaction between a wheel and a corrugated rail, *European Journal of Mechanics A/Solids*, **20**, 4, 673-684
2. IGELAND A., ILIAS H., 1997, Rail head corrugation growth predictions based on non-linear high frequency vehicle/track interaction, *WEAR*, **213**, 1/2, 90-97
3. ILIAS H., 1996, Nichtlineare Wechselwirkungen von Radsatz und Gleis beim Überrollen von Profilstörungen, *VDI Fortschritt-Berichte ser. 12*, **297**, VDI-Verlag, Düsseldorf
4. JOHNSON K.L., 1985, *Contact Mechanics*, Cambridge University Press
5. KALKER J.J., 1991, *Three-Dimensional Elastic Bodies in Rolling Contact*, Kluwer Academic Publisher
6. KOWALSKA Z., 2004, Vibro-impact motion of heavily loaded compact hard bodies, *Engineering Transactions*, **52**, 1/2, 37-55
7. NAYAK P.R., 1972, Contact vibrations, *Journal of Sound and Vibration*, **22**, 3, 297-322
8. NIELSEN J., IGELAND A., 1995, Vertical dynamic interaction between train and track – influence of wheel and track imperfections, *Journal of Sound and Vibration*, **187**, 5, 825-839
9. STRONGE W.J., 2000, *Impact Mechanics*, Cambridge University Press

Wibro-uderzenia wywołane przez nieregularne powierzchnie toczne szyn i kół kolejowych

Streszczenie

Nierówności na powierzchniach tocznych zwartych, lokalnie odkształcalnych ciał powodują drgania kontaktowe, w szczególności tak zwane wibro-uderzenia. Modelowanie, symulacja i analiza takiego wymuszenia oraz dynamicznej odpowiedzi na nie są przedmiotem badań. Analiza parametryczna przejściowych wibro-uderzeń wywołanych przez pojedynczą nierówność szyny jest pomocna w zrozumieniu dynamicznych własności układu. Ponadto, może być przydatna w projektowaniu eksperymentu diagnostyki defektów powierzchni tocznych oraz sąsiednich struktur dynamicznych, tj. zawieszenia i/lub toru. Symulacje wykonane z wykorzystaniem prostego modelu o jednym stopniu swobody zostały następnie porównane z symulacjami ruchu całego wagonu za pomocą programu Adams/Rail.

Manuscript received February 21, 2007; accepted for print April 4, 2007